This online publication has been corrected. The corrected version first appeared at thelancet.com/neurology on Aug 10, 2022

letter could have been based on misconceptions. The authors state that two systematic reviews[2,3] from our research group conclude that exercise training is not associated with neuroprotection. To clarify, the first systematic review[2] explicitly states that the evidence on the effects of physical exercise on brain volume in neurodegenerative populations appears sparse and inconclusive, most likely due to the absence of large, long-term (≥1 year), and well-designed studies. Moreover, the arguments put forward by Sandroff and colleagues[1] are the same as those outlined in the discussion of our first systematic review.[2] Hence, in the first review, according to the purpose of systematic reviews, we accurately described the existing literature and summarised the evidence leading to a balanced discussion that can help guide the direction and quality of future studies.

As for our second systematic review,[3] Sandroff and colleagues[1] appear to have overlooked its aim to summarise the existing evidence on the effects of exercise training on neurotrophic factors. Although we did note increased chronic levels of BDNF in patients with multiple sclerosis, this increase did not translate into neuroprotection in the few studies examining these levels.

Additionally, Sandroff and colleagues[1] imply that a randomised controlled trial from our group[4] did not involve a priori determined brain regions of interest for studying exercise-induced neuroprotection and relied on structural neuroimaging for generating conclusions on neuroprotection. To clarify, predefined regions of interest were registered at ClinicalTrials.gov (NCT02661555) and we applied extensive state-of-the-art diffusion kurtosis imaging in addition to volumetric neuroimaging.

We fully agree with Sandroff and colleagues[1] that a shift in scientific paradigm is slow and arduous, and that large randomised controlled trials are needed assessing the effect of exercise on neuroprotection in people with multiple sclerosis. We emphasised and thoroughly outlined this scientific paradigm shift in our 2019 review.[5]

As should be clear from our publications, we are strong advocates for exercise and its potential for eliciting neuroplasticity and neuroprotection in people with multiple sclerosis, yet we insist on balanced, evidence-based conclusions and recommendations. We encourage and welcome other research groups to help unravel the potential of exercise in multiple sclerosis, as we believe that a joint collaborative research approach is crucial.

UD has received teaching honorarium from Meyers Squib, Roche, and Biogen Idec. LGH, ML-C, and ES declare no competing interests.

*Lars G Hvid,
Martin Langeskov-Christensen,
Egon Stenager, Ulrik Dalgas
lhvid@ph.au.dk

Exercise Biology, Department of Public Health, Aarhus University, Aarhus, Denmark (LGH, ML-C, UD); The Danish MS Hospitals, Ry and Haslev, Denmark (LGH); Department of Regional Health Research, University of Southern Denmark, Odense, Denmark (ES); MS Clinic of Southern Jutland, Department of Neurology, Sønderborg, Denmark (ES)

1 Sandroff BM, Motl RW, Yong VW, Cutter GR, Giovannoni G. Exercise training in multiple sclerosis. *Lancet Neurol* 2022; **21:** 313.
2 Hvid LG, Harwood DL, Eskildsen SF, Dalgas U. A critical systematic review of current evidence on the effects of physical exercise on whole/regional grey matter brain volume in populations at risk of neurodegeneration. *Sports Med* 2021; **51:** 1651–71.
3 Diechmann MD, Campbell E, Coulter E, Paul L, Dalgas U, Hvid LG. Effects of exercise training on neurotrophic factors and subsequent neuroprotection in persons with multiple sclerosis—a systematic review and meta-analysis. *Brain Sci* 2021; **11:** 1499.
4 Langeskov-Christensen M, Grøndahl Hvid L, Nygaard MKE, et al. Efficacy of high-intensity aerobic exercise on brain MRI measures in multiple sclerosis. *Neurology* 2021; **96:** e203–13.
5 Dalgas U, Langeskov-Christensen M, Stenager E, Riemenschneider M, Hvid LG. Exercise as medicine in multiple sclerosis-time for a paradigm shift: preventive, symptomatic, and disease-modifying aspects and perspectives. *Curr Neurol Neurosci Rep* 2019; **19:** 88.

Interferon receptor dysfunction in a child with malignant atrophic papulosis and CNS involvement

Malignant atrophic papulosis is a rare, thrombo-obliterative vasculopathy, with either a cutaneous benign presentation or a systemic severe presentation, predominantly affecting the gastrointestinal tract, lungs, and CNS.[1] We report a heterozygous de-novo variant in the interferon α/β receptor subunit 1 gene (*IFNAR1*, MIM_107450) in a girl with malignant atrophic papulosis and CNS involvement who presented to our clinic in August, 2019, at age 9 years. Interferon signalling is dysregulated in our patient, and treatment with the Janus kinase 1/2 inhibitor baricitinib, and with anifrolumab (an antibody that blocks interferon signalling), has led to stabilisation of her signs and symptoms.

The patient is the only child of non-consanguineous, healthy, White, European parents. Pregnancy, delivery, and early childhood were uneventful. She had periodic holocephalic headaches at age 5 years. Bilateral glaucoma and signs of optic nerve atrophy were first diagnosed at age 6·5 years at another institution, requiring five surgical interventions (four trabeculectomies with mitomycin and a scleral patch), which took place within 1 year of the diagnosis, but did not stop the progression of glaucoma.

At age 7 years, the patient had multiple round, white skin lesions, 1–2 mm in diameter and with telangiectatic rims, disseminated on her entire integument. A skin biopsy showed a superficial perivascular dermatitis with traits of vasculopathy, but without signs of vasculitis (figure 1).

Acoustic evoked potentials were pathological at age 7·5 years; however, hearing loss in the right ear was not noticed until about 1 year later.

MRI results at age 7·6 years were unremarkable. Acute diplopia due to right-sided abducens paresis occurred at age 7·8 years, and left-sided ptosis and anisocoria (left larger than right) were detected 4 months later. The patient's hearing kept worsening and she had bilateral sensorineural inner ear damage, requiring hearing aids, by age 9 years. The patient's visual acuity also worsened, leading to bilateral blindness by age 10 years.

At age 8 years, the patient developed acute and progressive distal muscle weakness of both feet that spread to the legs, which within a few weeks also affected the hands and then the arms. She developed a neurogenic bladder and bowel dysfunction. Subsequently, the patient progressively lost the ability to walk, and her muscle weakness worsened and resulted in tetraplegia. Additionally, the patient reported hypersensitivity in her arms and head, and hyposensitivity in her legs. Electrophysiological studies revealed a peripheral demyelinating neuropathy at age 9·5 years. The patient had epilepsy with focal-onset seizures. Her parents reported that she had forgetfulness, as well as cognitive concerns, but a standardised test conducted at another institution when the patient was 10 years of age showed normal results.

A cranial MRI (figure 1) at 9 years of age showed multiple T2 hyperintensities, calcifications (confirmed by CT), and microbleeds, partly with contrast enhancement,

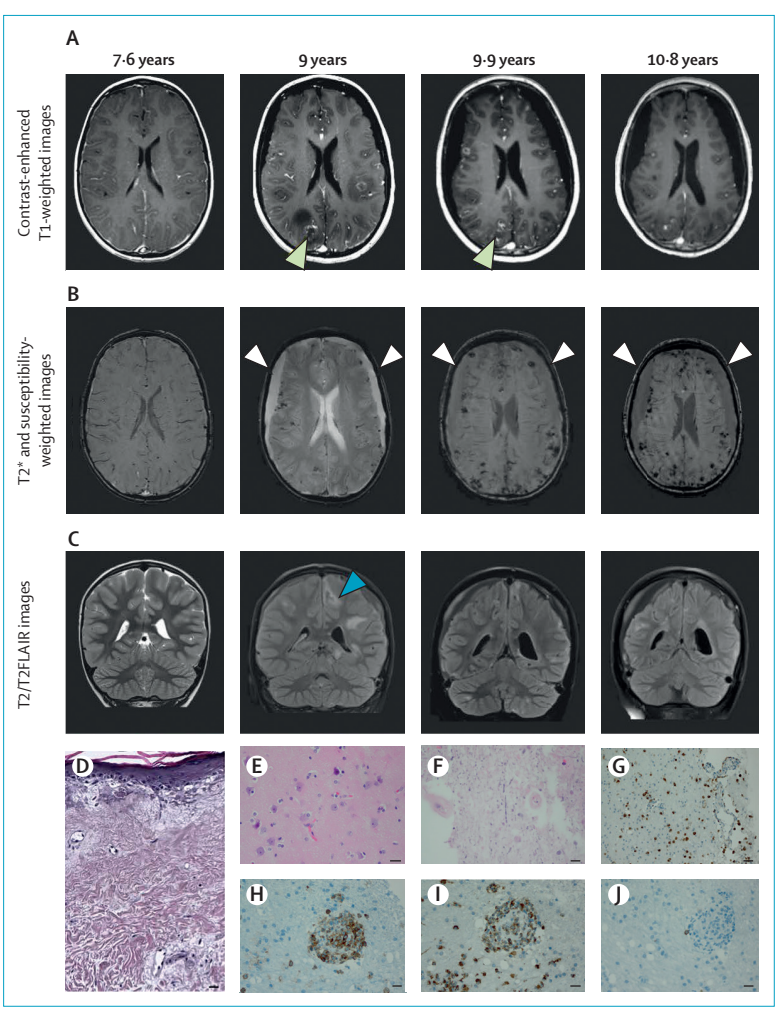

Figure 1: **MRI scans, histological analyses of the skin, and brain biopsy specimens**
(A) Contrast-enhanced T1-weighted images, (B) T2* (second column) and susceptibility-weighted images (first, third, and fourth columns), and (C)T2/T2FLAIR images of the brain at four timepoints: before our assessment (age 7·6 years, first column), before treatment (age 9 years, second column), 9 months after starting treatment with baricitinib (age 9·9 years, third column), and during combined therapy with baricitinib and anifrolumab (age 10·8 years, fourth column). Contrast-enhanced T1-weighted images showed multiple nodular and ring-enhancing lesions, primarily in the cortical ribbon and the subcortical white matter (eg, in the right parietal lobe, green arrowhead) before treatment (age 9 years). At 9·9 years of age, under baricitinib and hydroxychloroquine treatment, the lesions were still present (green arrowhead). Regardless of therapy, multiple cortical and subcortical signal voids on T2* and susceptibility-weighted images occurred throughout the entire brain, partly within the contrast-enhancing lesions, but also outside in otherwise normal-appearing tissue (age 9 years and 9·9 years), representing calcifications. Bilateral hygromas were observed surrounding both hemispheres and slowly progressed during the course of the disease (age 9 years *vs* 10·8 years, white arrowheads), often seen in malignant atrophic papulosis. Calcifications and enhancing lesions are in parts surrounded by perifocal oedema (hyperintensities on T2 FLAIR images, age 9 years and 9·9 years) that were distinct before the anti-inflammatory treatment was initiated (eg, left and right parietal lobes, blue arrowhead, age 9 years *vs* 10·8 years). (D) Haematoxylin–eosin staining (magnification ×20, scale bar 50 μm) of a skin biopsy sample showed a slightly atrophic epidermis with a superficial, pale, relatively acellular dermal infarct area parallel to the surface epithelium and imitating cytoid bodies. Mucin deposition was not observed. Endovasculitis in deeper dermal vessels with endothelial cell hyperplasia complicated by thrombosis could be seen. (E) On haematoxylin–eosin stained slides obtained after a brain biopsy (magnification ×400, scale bar 20 μm), fragments of the dura mater showed broad calcification. The overall histoarchitecture of the cerebral cortex was intact and showed hypoxic changes to be expected after surgical resection. (F) An area of mineralised necrotic cerebral tissue was evident, mostly well separated from the intact tissue fragments. Patterns of mineralisation included filamentous and globular structures (haematoxylin–eosin staining, magnification ×400, scale bar 20 μm). (G–J) On immunohistochemical staining (magnification ×400, scale bar 20 μm), lymphocytes and macrophages ($CD68^+$) were visible in the cortex (G), infiltrating the adjacent CNS parenchyma (H–J), but were mostly localised around intraparenchymal small vessels. Panels show $CD68^+$ macrophages (G, I), $CD45^+$ leukocytes (H), and $CD8^+$ cytotoxic T-cells (J).

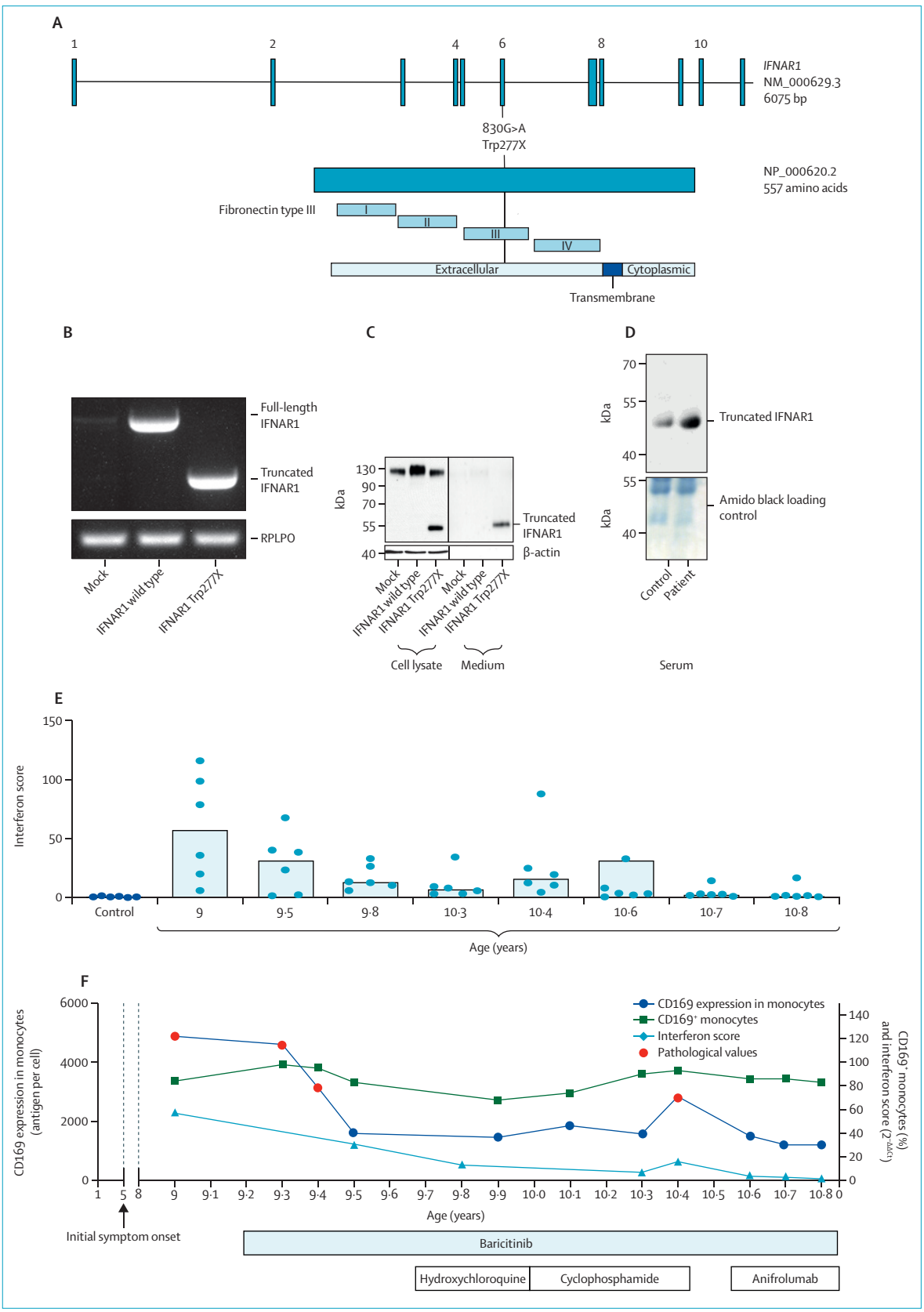
A
1
2
4
6
8
10
IFNAR1
NM_000629.3
6075 bp
830G>A
Trp277X
NP_000620.2
557 amino acids
Fibronectin type III
I
II
III
IV
Extracellular
Cytoplasmic
Transmembrane
B
Full-length IFNAR1
Truncated IFNAR1
RPLPO
Mock
IFNAR1 wild type
IFNAR1 Trp277X
C
kDa
130
90
70
55
40
Truncated IFNAR1
β-actin
Mock
IFNAR1 wild type
IFNAR1 Trp277X
Cell lysate
Medium
D
kDa
70
55
40
Truncated IFNAR1
Amido black loading control
Control
Patient
Serum
E
Interferon score
150
100
50
0
Control
9
9·5
9·8
10·3
10·4
10·6
10·7
10·8
Age (years)
F
CD169 expression in monocytes (antigen per cell)
6000
4000
2000
0
CD169 expression in monocytes
CD169+ monocytes
Interferon score
Pathological values
CD169+ monocytes (%) and interferon score (2−ΔΔCt)
140
120
100
80
60
40
20
0
1
5
8
9
9·1
9·2
9·3
9·4
9·5
9·6
9·7
9·8
9·9
10·0
10·1
10·2
10·3
10·4
10·5
10·6
10·7
10·8
Age (years)
Initial symptom onset
Baricitinib
Hydroxychloroquine
Cyclophosphamide
Anifrolumab

and predominantly subcortical and juxtacortical in the frontal and parietal lobes, in the corpus callosum, and in the cerebellar peduncles. A spinal MRI showed T2 hyperintensities over the entire length of the spinal cord. Multiple MRIs (figure 1) over the course of the patient's disease have revealed an increasing number of contrast-enhancing nodules, progressive oedematous and gliotic regions, and microbleeds and calcifications. The patient eventually developed bilateral hygromas, which were present at age 9 years.

Repeated CSF analyses showed high protein concentrations (about 24-times more than the normal range) without intrathecal antigen synthesis, antineuronal antibodies, or pathogens. The concentration in CSF of neopterin was also increased (2 µg/L; normal range <1·4 µg/L). A brain biopsy of a right frontal cortex lesion and dura at age 9 years showed severe mineralisation of the dura and reactive abnormalities with necrosis within the brain, and mild inflammatory infiltrates in the adjacent CNS parenchyma.

In summary, our patient, who is currently 12 years of age, has a combination of a cerebral phenotype (cognitive impairment, motor dysfunction, and cranial nerve involvement), a spinal phenotype (bowel and bladder involvement and tetraplegia), and peripheral neuropathy (hyperesthesia and reduced fine motor skills). Furthermore, cardiological assessment showed a repolarisation disorder, mildly decreased left ventricular function (left ventricular ejection fraction 53%), and mitral valve prolapse without cardiac decompensation. At age 10·4 years, the patient developed intermittent arterial hypertension, and cardiac MRI revealed severe myocardial oedema in the basal to midventricular lateral heart wall (appendix p 4). Sonography of the abdomen at age 8 and 10·4 years detected hyperechogenic lesions in the left kidney with normal function and perfusion.

By whole-exome sequencing of the patient and both unaffected parents, we identified a heterozygous de-novo variant, 830G>A (NM_000629.2, chr21:34721438G>A), in the patient's *IFNAR1* gene. At the protein level, the variant leads to a stop codon at position 277 (NP_000620.2; Trp277X), predicted to result in a truncated IFNAR1 protein, without the transmembrane and cytoplasmic domains responsible for signal transduction (figure 2A; appendix pp 1, 4). We hypothesised that this variant could encode a truncated and soluble IFNAR1 protein resembling a previously described IFNAR1 isoform derived from alternative splicing that can act as an interferon-signalling agonist.[2]

In cultured C20 human microglial cells ectopically expressing mutant *IFNAR1*, mRNA expression of truncated IFNAR1 was detected by RT-PCR, and truncated IFNAR1 protein was also detected in cell lysates and supernatant by western blotting (figure 2B, C). Similarly, we detected the truncated IFNAR1 protein in the patient's serum by immunoblotting, showing that the Trp277X *IFNAR1* variant resulted in a soluble form of IFNAR1 (figure 2D). Laboratory analyses of whole blood revealed a severely elevated interferon score (representing the median fold change [$2^{-\Delta\Delta Ct}$] in expression of six interferon-stimulated genes [*IFI27*, *IFI44L*, *IFIT1*, *ISG15*, *RSAD2*, and *SIGLEC1*], as measured by quantitative RT-PCR, normalised to the housekeeping gene *HPRT1* and compared with a control; PAXgene Blood RNA Tubes, Qiagen, Venlo, Netherlands; figure 2E; appendix p 1). Additionally, increased CD169^{+} monocytes and increased CD169 (SIGLEC1) expression on monocytes were detected (figure 2F). The addition of patient's serum to C20 cells increased their interferon signature, suggesting that Trp277X IFNAR1 drives the interferon dysregulation. In line with other experimental findings that revealed dysregulated interferon signalling, high expression of interferon-stimulated genes were recapitulated in cultured T cells from our patient (appendix pp 5–6). Addition of anifrolumab, an antibody targeting the extracellular part of IFNAR1, normalised the dysregulated interferon induction (appendix pp 5–6).

At age 7 years, the patient received methylprednisolone pulse therapy (30 mg/kg per day). Her disease progressed despite one treatment with intravenous immunoglobulin (2 mg/kg), five cycles of plasmapheresis, two doses of rituximab (375 mg/m²), and tocilizumab (200 mg every 2 weeks from age 8 to 9 years).

At first presentation to our centre (age 9 years), the patient received aspirin (50 mg/day) and levetiracetam (40 mg/kg per day). Because of her

See **Online** for appendix

Figure 2: **De-novo variant in the *IFNAR1* gene and experimental findings**
(A) Position of the identified variant in the gene and protein. (B, C) Following ectopic expression of wild-type or mutant (Trp227X) IFNAR1 in cultured C20 human microglial cells, mRNA expression of both IFNAR1 forms was detected by semi-quantitative RT-PCR with RPLPO as loading control (B), and protein expression of both forms was detected in cell lysates and in the medium by western blotting using antibodies specific for IFNAR1, with β-actin as a loading control (C). (D) In a serum sample from the patient, a signal of the expected size (~40 kDa) was detected by immunoblotting, whereas serum from a healthy donor showed a slightly slower-migrating, faint IFNAR1 variant. (E) The patient's interferon score (median fold change [$2^{-\Delta\Delta Ct}$] in mRNA expression of six interferon-stimulated genes [*IFI27*, *IFI44L*, *IFIT1*, *ISG15*, *RSAD2*, and *SIGLEC1*, each represented by a point on the graph] relative to the reference gene *HPRT1*) was elevated compared with the control (the patient's mother) and decreased after treatment initiation. (F) Overview of the patient's interferon signature and treatment timeline. Symptoms initially developed at around age 5 years. After several years of clinical progression, baricitinib treatment was started at around 9·25 years of age, resulting in a decrease in the expression of CD169 (SIGLEC1) on monocytes, a decrease in CD169^{+} monocytes, and a decrease in interferon score. After initiation of an additional immunomodulatory regimen (hydroxychloroquine and cyclophosphamide), the interferon score decreased further. However, after increases in CD169 expression on monocytes and the interferon score under cyclophosphamide treatment, cyclophosphamide was stopped and anifrolumab was added instead, which led to clinical stabilisation.

rapid disease progression and evidence of increased interferon pathway activation, we initiated off-label oral treatment with baricitinib (initial dose 0·025 mg/kg per day [0·5 mg/day]). We increased baricitinib weekly by 0·5 mg/day, up to 0·4 mg/kg per day (8 mg/day in four single doses). In view of the clinical and laboratory similarities between interferonopathies and the condition of our patient, we chose the Janus kinase 1/2 inhibitor baricitinib because of its beneficial effects in interferonopathies.[3,4] This treatment led to clinical stabilisation after a few weeks, disappearance of the skin lesions, and stabilisation of MRI findings (figure 1). However, after 8 months, partial progression occurred when the patient developed increased weakness of her head and trunk muscles. We added oral hydroxychloroquine (4 mg/kg per day [100 mg/day]; figure 2F), which was discontinued after 4 months because of disease progression. After hydroxychloroquine was discontinued, we added low-dose cyclophosphamide (25 mg/m^2 per day), which we discontinued after 4 months due to disease progression and sleepiness. We then started off-label therapy with the monoclonal IFNAR1 inhibitor anifrolumab, which has been developed for (but not yet approved in) adults with systemic lupus erythematosus.[5] Because no data are available on the dosage of anifrolumab in children (in adults, dosage is 300 mg intravenously every 4 weeks), we initiated treatment with 200 mg every 4 weeks. However, after the third 200 mg dose, we reduced the dose to 150 mg because the patient had pneumonia requiring hospitalisation. The patient had a spontaneously resolved episode of fever and increased C-reactive protein, without identification of a cause, 3 days after the fourth 150 mg dose of anifrolumab. Co-treatment with baricitinib and anifrolumab resulted in a rapid clinical, radiological, and laboratory improvement, with better cognitive abilities and muscle strength.

The patient's interferon score and CD169 expression on monocytes normalised after baricitinib initiation, increased under co-medication with cyclophosphamide, and decreased again after cyclophosphamide was stopped. Interferon scores were lowest under co-medication with baricitinib and anifrolumab (figure 2F).[6]

In conclusion, this case underlines the contribution of type I interferon signalling to malignant atrophic papulosis with CNS involvement and provides evidence that the disease can be caused by a gain-of-function *IFNAR1* variant. Treatment with baricitinib and anifrolumab effectively slowed disease progression. A randomised controlled trial of baricitinib or anifrolumab, or a combination, in genotyped patients with malignant atrophic papulosis might be warranted.

EK has received grants from the German Research Foundation (SFBTR 167 Neuromac, RTG2719 PRO). CCZ has participated on advisory boards for Bayer Healthcare, GlaxoSmithKline/Stiefel, Incyte, Inflarx, Janssen, L'Oréal, NAOS-Bioderma, Novartis, Pierre Fabre, PPM-Medical Holding, Regeneron, Sobi, UCB Pharma,and AbbVie; received payment for lectures from AbbVie, NAOS-Bioderma, Pierre Fabre, PPM-Medical Holding, Sobi, and Amgen; payment for expert testimony from Accure Acne, Luvis, and Relaxera; and has participated in research studies for AbbVie, Advanced Oxygen Therapy Inc, Astra Zeneca, Bristol-Myers Squibb, Celgene, Galderma, Inflarx, NAOS-Bioderma, Novartis, PPM-Medical Holding, Relaxera, and UCB Pharma, all unrelated to the submitted work. CCZ is also an unpaid board member of the European Academy of Dermatology and Venerology, International Society for Behcet's Disease, European Hidradenitis Suppurativa Foundation, and Deutsches Register Adamantiades Behcet. AMK has participated on advisory boards for GW Pharmaceuticals and Novartis; received payment for presentations from GW Pharmaceuticals and Ethypharm; and received consulting fees from GW Pharmaceuticals, Avexis, and Ethypharm, all unrelated to the submitted work. AMK has also and received grants from the German Research Foundation (SFB1315, FOR3004). L-LB, FE, and DH declare no competing interests. This study was supported by the Einstein Stiftung Fellowship through the Günter Endres Fond. Other contributors' competing interests are shown in the appendix.

**Lena-Luise Becker†, Frédéric Ebstein†, Denise Horn, Christos C Zouboulis, Elke Krüger†, Angela M Kaindl†, on behalf of the IFNAR1 Research Group‡*
angela.kaindl@charite.de

†Contributed equally.

‡Additional contributors are listed in the appendix.

Department of Pediatric Neurology (L-LB, AMK), Center for Chronically Sick Children (L-LB, AMK), Institute for Cell Biology and Neurobiology (L-LB, AMK), and Institute of Medical Genetics and Human Genetics (DH), Charité–Universitätsmedizin Berlin, 13353 Berlin, Germany; Institute of Medical Biochemistry and Molecular Biology, Greifswald University Medicine, Greifswald, Germany (FE, EK); Faculty of Health Sciences, Brandenburg Medical School Theodor Fontane, Dessau, Germany (CCZ); Departments of Dermatology, Venerology, Allergology, and Immunology, Dessau Medical Center, Dessau, Germany (CCZ)

1 Theodoridis A, Konstantinidou A, Makrantonaki E, Zouboulis CC. Malignant and benign forms of atrophic papulosis (Köhlmeier-Degos disease): systemic involvement determines the prognosis. *Br J Dermatol* 2014; **170:** 110–15.

2 Han CS, Chen Y, Ezashi T, Roberts RM. Antiviral activities of the soluble extracellular domains of type I interferon receptors. *Proc Natl Acad Sci USA* 2001; **98:** 6138–43.

3 Sanchez GAM, Reinhardt A, Ramsey S, et al. JAK1/2 inhibition with baricitinib in the treatment of autoinflammatory interferonopathies. *J Clin Invest* 2018; **128:** 3041–52.

4 Meesilpavikkai K, Dik WA, Schrijver B, et al. Efficacy of baricitinib in the treatment of chilblains associated with Aicardi-Goutières syndrome, a type I interferonopathy. *Arthritis Rheumatol* 2019; **71:** 829–31.

5 Peng L, Oganesyan V, Wu H, Dall'Acqua WF, Damschroder MM. Molecular basis for antagonistic activity of anifrolumab, an anti-interferon-α receptor 1 antibody. *MAbs* 2015; **7:** 428–39.

6 Orak B, Ngoumou G, Ebstein F, et al. SIGLEC1 (CD169) as a potential diagnostical screening marker for monogenic interferonopathies. *Pediatr Allergy Immunol* 2021; **32:** 621–25.

Time to revise primary prevention guidelines for stroke and cardiovascular disease

Strategies for prevention of cardiovascular disease that are based on risk assessment and targeted to high-risk populations (ie, the so-called high-risk approach) are thought to deliver large benefits and to be cost-effective, compared with population-wide strategies.[1] According to this high-risk approach, management guidelines for blood pressure and cholesterol must be based on the use of an individual's predicted absolute risk of cardiovascular disease as the threshold for drug therapy. However,